JP2.7

POLARIMETRIC RADAR OBSERVATIONS OF THE STRUCTURE OF TROPICAL CYCLONE INGRID

Peter T. May[1] and T.D. Keenan

BMRC, Melbourne, Australia

1. INTRODUCTION

The structure and intensity of tropical cyclones around landfall are a major topic of research because of the potential impact on human populations and property. Polarimetric weather radars offer the possibility of much more accurate measurements of rainfall and the precipitation microphysical structure of storms nearing landfall. These are key issues relating to the impact of tropical storms. Polarimetric capabilities are a key component on the planned upgrade of the US weather radar network. There are several research radars with this capability, but there have not been TC observations published. In March 2005, an intense tropical cyclone, TC Ingrid moved within 100 km of the Darwin research polarimetric radar (Keenan et al., 1998). Ingrid was a long lived storm that reached Category 5 intensity as it crossed the North Queensland coast, re-intensified over the Gulf of Carpentaria and then moved along the north coast of Australia along the monsoon trough where it lost some intensity, but remained a severe tropical cyclone. It then moved into the Timor Sea where it again re-intensified before recurving and making its final landfall. While this storm did not cross the coast near Darwin, it did propagate along an extended section of east-west oriented coastline with the circulation centre right on the coastline. As will be shown, this resulted in some remarkable asymmetries in the storm structure. The best track estimates of the central pressure when it was in radar range had the storm filling from 950 hPa to 970 hPa and an analysed intensity dropping from a Category 4 storm to Category 3. The radial wind speeds estimated near the eye wall at low elevations at the time of closest approach to the radar, but still about 1.8 km above the ground were ~ 52ms^{-1} consistent with the Category 3 rating. This paper will describe the rainfall and microphysical structure of this storm as it moved past the radar at a speed of about 3.5 ms^{-1}.

1. *Corresponding author address*: Dr. P. May
Bureau of Meteorology Research Centre
GPO Box 1289 Melbourne, Vic. 3008
p.may@bom.gov.au

2. POLARIMETRIC RADAR

A polarimetric weather radar differs from conventional Doppler radar by its ability to transmit and receive on different polarisations. In the case of the 5.5 cm wavelength Darwin C-Pol radar, alternate pulses of horizontal and vertically polarised radiation are sent and received. Detailed descriptions of the enhanced capabilities associated with such systems can be found in Zrnic and Ryzhkov (1999), but the germane issue here is the capability for much greater accuracy of rainfall estimates and the ability to estimate the microphysical characteristics of the precipitation. The microphysical classification follows the fuzzy logic approach of Straka et al (2000). These retrievals have found good validation in thunderstorm data (May and Keenan, 2005). It should be noted that the large velocities caused considerable aliasing and also appeared to impact some of the data quality in the eye-wall region, probably due to the large spectral widths associated with intense convection and transverse (to the beam) velocities. However, the results presented here show spatial and temporal consistency.

3. CORE STRUCTURE

As shown in Fig. 1, TC Ingrid passed along the north coast of Australia and was decreasing in intensity as it passed the Tiwi Islands. An IR satellite image at 0700 UT on March 13 (Fig. 2) shows continuous cloud coverage with no clear eye. The cold IR temperatures are concentrated on the north and down wind side of the eye circulation along with some evidence of deep convection in parts of the rainbands.

A radar scan at 0730 UTC (Fig. 3) shows the very asymmetric reflectivity structure about the storm centre with the maximum reflectivity on the north (off-shore) side consistent with the satellite imagery. This asymmetry persisted for the entire storm passage (> 12 hours) past the islands and is reflected in the total rainfall estimated from the polarimetric data (Fig. 4). The time for a cell to be advected around the entire eye is ~ 1 hour,

so the relatively steady state of the convective asymmetry is noteworthy. This resulted in a very asymmetric rainfall distribution, with totals of more than 500 mm off-shore and much less, but still significant totals on the islands and mainland associated with rainbands and the southern part of the eyewall.

The radar cross-sections through the eyewall (Fig. 5) show that the intense side is always characterized by echo tops in the vicinity of 18-20 km, i.e. the convection on the north side of the eye is reaching to the tropopause and overshooting while the reflectivity structure on the south side is not only much shallower, but seems to be feeding into the outflow mask between altitudes of 10 and 15 km. This altitude range is consistent with the anticyclonic outflow in Darwin sounding data. The outflow layer includes a layer over the central eye which does not show clearly in the satellite imagery. The radar observations are consistent with the satellite imagery showing the coldest cloud top temperatures to the north, but also some cyclonic rotation of the cold temperatures around to the eastern side of the storm. This is not necessarily inconsistent with the radar data that does not show anywhere near as much rotation, as it may be explained by the radar reflectivity being dominated by large ice crystals that fall out relatively quickly.

The polarimetric radar also allows us to estimate the precipitation microphysical structure. Fig 5 shows the micro-physical structure in a north-south cross-section through the storm. In the intense convection in the eyewall there appears to be an almost continuous volume of rain/hail mixtures in the region between 3 and 5 km in altitude with a substantial volume of wet graupel over-lying this. This is indicative of the strong updrafts in the high reflectivity area. The remainder of the eyewall convection and the shallow cells visible south of the eyewall, which are associated with the small rainbands visible in Fig 3, do not show any substantial mixed phase regions. Interestingly, where there is intense convection in the rainbands, mostly after the bands cross onto the land, there are rain/hail mixture regions produced.

Fig 6 shows a cross-section of radar reflectivity and radial velocity across the storm. The reflectivity shows the higher reflectivity present in the northern side of the eyewall clearly and that there remained echoes of about 25 dBZ and evidence of a brightband extending across the eye indicating some drizzle. The velocity cross-section shows the maximum velocities of about 50 ms^{-1} and a radius of maximum wind of 20 km slightly inside the highest reflectivity. There is also some asymmetry in the radial dependence. On the north-west side the radial velocity initially falls of as the radius, $R^{-1/2}$ with a transition to a 1/R dependence, which is inertially neutral, between the eyewall and the first rainband. On the southeast side, downwind from the major convection the fall-off was mid-way between these dependencies.

4. RAINBAND STRUCTURES

There were two distinct types of rainbands observed in the radar data. There were some large scale, long lived bands that extended from near the eyewall on the north side around south of Darwin and a similar, but less well developed line that connected to the south-west side of the eyewall. These lines were almost stationary. The band was largely stratiform in nature except for some embedded convective elements. These were mostly, but not always initiated near coastal boundaries where there is an increase of surface friction and therefore an updraft triggered. The convection in these elements was often deep, reaching to the tropopause and with rain/hail mixtures detected between heights of 3 and 5 km.

In contrast, there were a number of small lines with a length of about 50 km within a radius of about 60 km. Several of these can be seen in Fig 3 including one that is intensifying significantly. As can be seen in the cross-section, these were often made up of shallow cells. These rotated about the storm much faster than the outer bands before stalling and merging near the intersection of the large band. It is not clear if these lines were propagating with respect to the storm circulation, but their regularity certainly gives them a wave-like appearance. The reflectivity in these bands reached reasonably high values, 40-45 dBZ, as can be seen in Figs 3, 4 and 6 but tended to be shallow as the echoes were confined mainly below the freezing level.

5. DISCUSSION AND CONCLUSIONS

The most dramatic feature of the cross-sections and rainfall in the region of the eye is the persistent asymmetry in the eyewall height and intensity. Interestingly this was on the ocean side of the vortex centre, rather than over land. It may be thought that the increase in surface roughness on the on-shore flow would have enhanced the local convergence and hence rain on the land side of the islands, but the reverse patter is evident. You do see a triggering effect of convection on landfall in some of the rainband structure. Another clear feature on the south side is the spinning off of small wave-like rainbands.

This paper represents the first documentation of tropical cyclone microphysical structure with a

polarimetric radar. A particular feature is the volume where hail is forming, but not reaching the surface around the eyewall and in some of the more intense cells of the rainbands. There is also an extensive region of wet graupel overlaying the hail. These are consistent with the strong up-drafts present in the deep convection. Note that soundings from Darwin showed a typical near–cyclone sounding that was almost moist adiabatic and high humidity through its depth with little CAPE or convective inhibition. This also makes the weakness of the eye over the islands puzzling – but it appears the moisture availability over the ocean was a key (e.g. Chan et al, 2004). Another possibility is a delay while the cells developed as they rotated over the land, but there was no clear signature of this around the eyewall.

The outflow from the storm had substantial radar echoes between 10 and 14 km in elevation and was composed mostly of snow with a tendency for larger or denser crystals with higher reflectivities near the lower parts of the cloud (Fig. 5). This outflow extended well past the eye, at least for a radius of 70 km, and covered part of the eye-itself, although the height of the reflectivity contours was a minimum in the eye. The satellite image showed a dense overcast over the whole storm at this time consistent with the radar images. The eye only cleared after the storm had moved past the islands and was in the open ocean.

The right-hand asymmetry observed here is an extreme case of what has often been observed as storms are making landfall. For example, papers by Blackwell (2000) and Chan et al (2004) as well as references cited by those papers document convective maxima to the left of northern hemisphere storms as they are making landfall, although models tend not to produce this result. The long lifetime of the asymmetry and the propagation along a coast rather than perpendicular to the coast may make this a good test for models.

References

Blackwell, K.G., 2000: The evolution of Hurricane Danny (1997) at landfall: Doppler-observed eyewall replacement, vortex contraction/intensification and low level wind maxima, *Mon. Wea. Rev.*, *128*, 4002-4016.

Chan, C.L., K.L. Liu, S.E. Ching and E.T. Lai, 2004: Asymmetric distribution of convection associated with tropical cyclones making landfall along the South China coast, *Mon. Wea Rev.*, **132**, 2410-2420.

Keenan, T.D., K. Glasson, F. Cummings, T.S. Bird, J. Keeler and J. Lutz, 1998: The BMRC/NCAR C-Band polarimetric (C-POL) radar system, *J. Atmos. Oceanic Tech.*, **15**, 871-886.

May,P.T. and T.D. Keenan, 2005: Evaluation of microphysical retrievals from polarimetric radar with wind profiler data, *J. Appl. Meteor.* **44**, 827–838.

Straka, J.M., D. Zrnic and A. Ryzhkov, 2000: Bulk hydrometeor classification and quantification using polarimetric radar data: Synthesis of relations. *J. Appl. Meteor.*, **39**, 1341-1372.

Zrnic, D.S. and A. Ryzhkov, 1999: Polarimetry for a weather surveillance radars, *Bull. Amer. Meteor. Soc.*, **80**, 389-406.

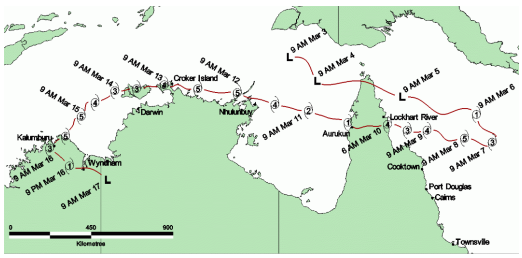

Figure 1 Official best track for TC Ingrid. Note that it was a long lived storm with several cycles of intensification depending on land influences.

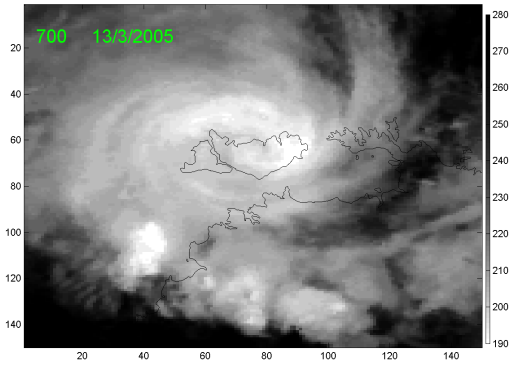

Figure 2 Geostationary satellite IR inage of TC Ingrid at 0700 UTC, March 13, 2005.

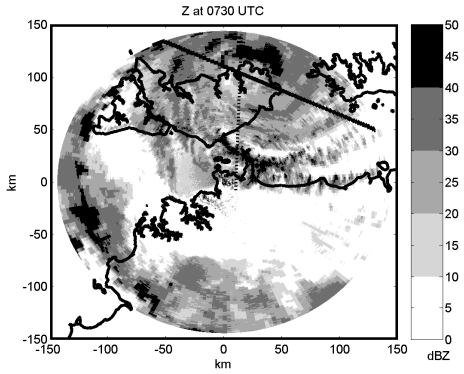

Figure 3 Radar reflectivity at an elevation angle of 0.5°at 0730 UTC, March 13, 2005. The solid line marks the cross-section of velocity and reflectivity through the eye and the dashed line the cross-section of reflectivity and microphysical classification. The storm centre is approximately at (100, 25) km. Note the asymmetries of the eye wall and the presence of several rain-bands

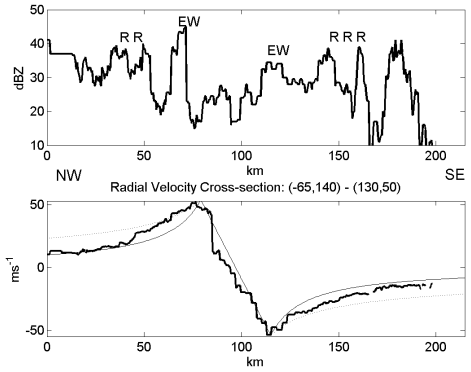

Figure 4 Cross-section of reflectivity (top) and radial velocity (bottom panel) along the solid line marked on Fig 3. The location of rainbands (R) and the eyewall (EW) are shown on the reflectivity. The radial velocity has an overlay of the expected profile for a vortex with a R^{-1} (light solid line) and $R^{-1/2}$ (light dotted line) radial dependence and linear inside the radius of maximum wind.

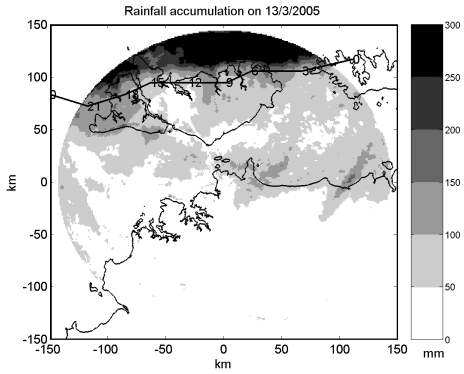

Figure 5 24 hour rainfall accumulations beginning 00 UTC on March 13, 2005 along with the storm best track and time of each fix. Note the impact of the storm asymmetry on the rainfall pattern.

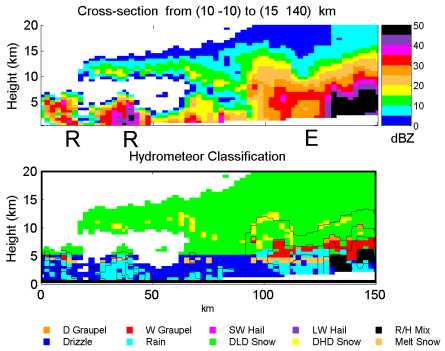

Figure 6 Quasi north-south cross-section of the radar reflectivity and polarimetric microphysical classification along the dashed line in Fig. 3. E marks the centre of the eye and R's rainbands.